Optimization of isocratic supercritical fluid chromatography for enantiomer separation

Chen Wenda, Reza Haghpanah, Arvind Rajendran *, Mohammad Amanullah

Nanyang Technological University, School of Chemical and Biomedical Engineering, 62 Nanyang Drive, Singapore 637459, Singapore

Abstract

This paper presents multi-objective optimization analysis and experimental implementation of a single column isocratic supercritical fluid chromatography process for the enantioseparation of flurbiprofen. The single column process is simulated using a detailed model with equilibrium description by a competitive Langmuir isotherm. The optimization problem has been formulated with the objectives of maximizing of productivity and minimizing solvent consumption under different product purity and recovery constraints. The solubility of the solute in the mobile phase is explicitly accounted in the problem formulation. The results showed a maximum productivity of 5 kg racemate/kg stationary phase / day with a corresponding organic solvent consumption of 80 L/kg racemate for a required purity and recovery of 95%. The optimal operating conditions have been experimentally implemented in an analytical scale laboratory set-up which support the optimization results.

Key words: Enantioseparation, Supercritical fluid chromatography, Multi-objective optimization, Flurbiprofen, Genetic algorithm

1 Introduction

The awareness that different enantiomers of a racemic compound may have different pharmacological effects makes chirality an important issue in the modern pharmaceutical industry. The toxicological and pharmacological properties of each enantiomer has to be tested during clinical trials as required by the regulatory authorities [1]. Further, single enantiomer drugs constitute about

* Corresponding author, Fax:+65- 6794 7553, Tel :+65 - 6316 8813
Email address: arvind@ntu.edu.sg (Arvind Rajendran).

40% of the total drug sales [2]. All of these provide the motivation to develop processes to obtain single enantiomers. Chromatography in both single and multi-column modes is an effective technique for preparative enantioseparation [3,4]. While most separations are performed using high performance liquid chromatography (HPLC), the method suffers from several drawbacks. Firstly, large pressure drops are encountered in HPLC when high throughputs are required. Large pressure drops cause stationary phase degradation and result in unexpected performance. Secondly, the desired component is collected as a dilute fraction and must be recovered from the mobile phase. This brings an extra step, e.g. evaporation, that makes the process expensive and time-consuming. Simulated moving bed chromatography (SMB), a multi column continuous process, reduces a number of the above limitations with increased productivity and reduced solvent consumption [4] . In any case, these processes involve the handling of large volume of solvents which translates into high energy consumption and associated disposal costs.

Supercritical fluid chromatography (SFC) is one of the most promising chromatographic methods in achieving fast enantioseparations with high productivity [5]. SFC uses supercritical fluids, such as CO_2, as mobile phase which has intermediate properties between gas and liquid. The viscosity of supercritical fluid is less than that of liquid and hence allows for the operation of preparative chromatographic columns at high flow rates with low pressure drops. This, in addition to the fact that the diffusion coefficients of solute in supercritical fluids are higher compared to liquid, reduces the batch separation time without compromising column efficiency thereby leading to increased productivity [6,7]. Rapid column equilibration after changes in chromatographic parameters reduces the time for method development. The solvent strength of a supercritical fluid is strongly influenced by the pressure. Hence pressure can be used as an additional degree of freedom to alter retention properties. SFC provides a distinct advantage also for fraction collection. By reducing the pressure of the mobile phase, CO_2 can be easily separated resulting in a concentrated product and effectively reducing recovery costs [7]. Shorter analysis and equilibration time, higher productivity and efficiency, less cost in disposal of solvent, all of these make SFC a competitive technology for enantioseparations. It is also worth noting that multi-column processes have been successfully demonstrated using supercritical fluids as mobile phase [8–10].

To purify large samples, there are usually two methods: scale up of system or column overloading. While scale-up of system involves using larger column diameter, higher flow rate, in column overloading the amount of injected sample is increased until the desired level of separation is achieved. To implement column overloading, high sample concentrations are required which is called concentration overloading. Concentration overloading is only possible when the solute has a good solubility in the mobile phase. Injection of samples whose concentrations are above the solubility limit can lead to precipitation,

thereby leading to pressure build up. To avoid this, the solubility of sample must be taken into account in preparative chromatography. While solubility measurements in liquids are straightforward, those in high pressure mixed supercritical phases are laborious. Hence for kilogram scale SFC separations, solubility measurements are seldom performed.

Systematic optimization of preparative SFC that maximizes the productivity and further decreases the solvent consumption is yet scarce in practice. This is primarily due to the large number of controllable instrumental and physicochemical parameters in SFC process, including flow rate, pressure, modifier composition, particle size and characterization of stationary phase. This study aims to address this issue. In this work, optimization of isocratic SFC for the enantioseparation of flurbiprofen has been undertaken using detailed mathematical models. Genetic algorithm has been used for the search of optimal operating conditions. Since both productivity and solvent consumption influence the economy of the SFC process, the optimization problem has been formulated as a multi-objective instead of a single objective optimization problem. The optimization studies have been done with actual experimental data under different purity and recovery constraints. In this study, the solubility of sample in supercritical mobile phase has been selected as a hard constraint and has been calculated based on experimental data published before [11]. Finally, two of the representative optimum operating conditions have been experimentally demonstrated on a laboratory scale SFC unit and results are reported.

2 System characterization

2.1 Materials and experimental set-up

Racemic flurbiprofen with a purity $\geq 99\%$ was obtained from Sigmal-Aldrich (Singapore). HPLC grade methanol (Aik Moh Paints and Chemicals, Singapore) was used as the modifier with carbon dioxide (purity: 99.8%, Singapore Oxygen Air Liquide, Singapore). An analytical Chiralpak AD-H column (250×4.6 mm, particle size: 5 μm) was used as the chiral stationary phase.

The set-up used for experiments has been reported earlier [12]. In short, two syringe pumps are used to deliver CO_2 and the modifier. A UV detector located at the column outlet provides the elution profile and a back pressure regulator located downstream of the detector controls the pressure in the unit. A detailed study that explores the effect of pressure and modifier composition on the adsorption equilibrium and mass transfer characteristic has also been reported [12]. Besides, data to account for the effect of flow rate on pressure

drop and efficiency and and isotherm parameters at higher concentrations were needed to carry out the optimization studies. These experiments are discussed below.In this study the temperature was maintained at 30°C. The back pressure was arbitrarily fixed at 135 bar. It was shown earlier that the selectivity and resolution did not show significant changes within the operating range and that the solubility was influenced more by the modifier composition than by pressure. Hence, the decision to fix the back pressure seemed reasonable.

2.2 Characterization of pressure drop

The pressure drop measurements at different flow rates and modifier concentrations were performed at a fixed back pressure of 135 bar. The measured pressure drops are plotted in Fig. 1. As expected, the pressure drop increased with increasing flow rate and modifier concentrations [13].

The pressure drop across the column in SFC can be described by the Darcy's law [14]:

$$\frac{\Delta P}{L} = -\beta \frac{(\rho v)\mu}{\rho} \tag{1}$$

where ρ and μ are the fluid phase density and viscosity respectively, the interstitial velocity is denoted by v and β is a the column permeability, that is typically fitted to experimental results. In the present work, although pressure drops up to 60 bar were measured, owing to the rather high modifier composition the change of density and viscosity with respect to change in pressure were marginal. Hence, average values of density and viscosity corresponding to the average pressure (arithmetic mean of inlet and outlet pressures) were used to regress the value of β. The fluid density was calculated using the Peng-Robinson equation of state along with a 2 parameter mixing rule. The fluid viscosity was calculated as weighted mole fraction average of the CO_2 and methanol viscosity [15]. The value of β=5.785×10^{-13} m mL^{-1} was regressed by minimizing the error between the experimental and calculated pressure drop. The calculated values of pressure drop are plotted in Fig. 1 and show an acceptable description of the experimental trends.

2.3 Characterization of HETP

The height equivalent to a theoretical plate (HETP) is a commonly used parameter to estimate column efficiency. Large values of HETP represent peak broadening that deteriorate separation. Operating conditions such as flow rate, mobile phase composition affect HETP. Previous studies have shown that pressure drops contribute to loss of efficiency in SFC when the mobile phase was

compressible [13,14]. In order to investigate these effects under SFC conditions, the HETP values were measured under different flow rates and modifier concentrations by injecting dilute sample of racemic flurbiprofen. As observed from Fig. 2, both flow rate and modifier composition had a minor effect on HETP over the range of operating conditions investigated in this work. Further, the value of HETP is rather small (around 10 μm) showing a high efficiency of the column. Such high column efficiency may be attributed to the high diffusivity of supercritical fluids and small particle size (5 μm) of stationary phase. Hence, in the entire study, the minor variation of HETP was not accounted for and assumed to be adequately described by the fitted mass transfer coefficients reported earlier [12].

2.4 Characterization of isotherm

The isotherm data used in this study was measured using the same method reported earlier [12]. Since the data reported in the previous study corresponded to lower concentrations, the isotherm parameters were re-estimated by using an injection loop of 100 μL. The injection concentrations chosen were close to the solubility limits in supercritical mixture (see Section 2.5). The classical Langmuir isotherm:

$$n_i^* = \frac{\Gamma_i K_i c_i}{1 + K_{\mathrm{R}} c_{\mathrm{R}} + K_{\mathrm{S}} c_{\mathrm{S}}} = \frac{H_i}{1 + K_{\mathrm{R}} c_{\mathrm{R}} + K_{\mathrm{S}} c_{\mathrm{S}}} \tag{2}$$

where Γ_i is the saturation capacity of the enantiomer and K_i is the component equilibrium constant. The Henry constant, H_i, was obtained by injections of dilute samples at a constant back pressure of 135 bar but under different modifier concentration, namely 13%, 18% and 20%. The following equation is used to represent Henry constant as a semi-empirical function of mobile phase density and modifier concentration [16]:

$$H_i = \frac{1}{a_i c_m + d_i} \left(\frac{\rho^o}{\rho} \right)^{p_i c_m + q_i} \tag{3}$$

where c_{m} is the modifier concentration in %(w/w), ρ and ρ^o are the density at operating and reference conditions respectively, while parameters a_i, d_i, p_i and q_i are empirical constants. The estimated value for the empirical constants are reported in Table 1. The saturation capacity, Γ_i, was calculated by the inverse method. It was found that the modifier composition had a minor effect on the Γ_i and hence average of values from the different runs was used as a representative value (see Table 1). Equations 3 together with values of Γ_i

provide the complete description of the isotherms for the region of interest. The use of average values gave adequate description of the experimental profiles.

2.5 Characterization of solubility

The solubility of flurbiprofen in pure CO_2 and in CO_2 + methanol was experimentally measured using a direct visualization technique [11]. The Peng-Robinson equation of state was used to describe the solubility over a wide range of modifier composition (upto 13% w/w). Since the modifier compositions used in the current study are larger than the ones reported, the interaction parameters were re-estimated based on the experimental data with the largest modifier composition, i.e., $c_{\mathrm{m}} = 13\%$ and the values of solubility for $c_{\mathrm{m}} > 13\%$w/w were calculated. The predicted solubility (σ) for $13 < c_{\mathrm{m}}(\mathrm{w/w}) < 20$ can be described by the empirical equation:

$$\sigma = 0.3196c_{\mathrm{m}}^2 + 0.5815c_{\mathrm{m}} - 8.6589. \tag{4}$$

3 Modeling of column dynamics

The dynamics of solute transport in the chromatographic column was represented by an axially dispersed plug flow model:

$$\frac{\partial c_i}{\partial t} = D_{ax,i}\frac{\partial^2 c_i}{\partial z^2} - \frac{\partial (c_i v)}{\partial z} - \frac{1-\epsilon}{\epsilon}\frac{\partial n_i}{\partial t} \tag{5}$$

where c_i and n_i are the concentrations of the solute i in the mobile phase and in the stationary phase respectively, v is the interstitial velocity, $D_{ax,i}$ is the axial dispersion coefficient and ϵ is the total porosity of the column.

In this study, the density change caused by pressure drop is less than 3% and therefore, the change of velocity arising due to the adsorption of the solute can be neglected. Under this assumption, Equation 5 can be written as:

$$\frac{\partial c_i}{\partial t} = D_{ax,i}\frac{\partial^2 c_i}{\partial z^2} - v\frac{\partial c_i}{\partial z} - \frac{1-\varepsilon}{\varepsilon}\frac{\partial n_i}{\partial t} \tag{6}$$

A linear driving force (LDF) model is used to describe the mass transfer from the fluid to the solid phase:

$$\frac{dn_i}{dt} = k_{f,i}(n_i^* - n_i) \tag{7}$$

where n_i^* is the concentration in the adsorbed phase in equilibrium with c_i.

The set of partial differential equations with suitable initial and boundary conditions were discretized in space using a finite difference scheme with 40 grid points per 1 cm of column length. The resulting set of ODEs were solved using the Gear's method as implemented in IMSL FORTRAN subroutines.

4 Process Optimization

4.1 Definition of parameters

Purity, recovery, productivity and solvent consumption are important parameters to evaluate the separation efficiency and quality. In this work, recovery (Y) and purity (P) are defined with respect to the individual fractions as:

$$\begin{aligned} Y_i &= \frac{\text{Amount of solute } i \text{ collected in the fraction}}{\text{Amount of solute i injected}} \\ &= \frac{Q\int_{t_i^{\text{start}}}^{t_i^{\text{end}}} c_i\, dt}{V_{inj,i}c_{inj,i}}, \qquad i = R, S \end{aligned} \tag{8}$$

$$\begin{aligned} P_i &= \frac{\text{Amount of solute } i \text{ collected in the fraction}}{\text{Total amount of two enantiomers collected in the same fraction}} \\ &= \frac{\int_{t_i^{\text{start}}}^{t_i^{\text{end}}} c_i\, dt}{\int_{t_i^{\text{start}}}^{t_i^{\text{end}}} (c_{\text{R}} + c_{\text{S}})\, dt}, \qquad i = R, S \end{aligned} \tag{9}$$

The symbols t_i^{start} and t_i^{end} denote the start and end time of collection for the fraction that is predominantly i. Note that in the simulations, the efficiency of fraction collection is considered to be 100%. In other words, all the solute that is to be collected between t_i^{start} and t_i^{end} are collected without any loss in the collection device, e.g. cyclone. The productivity (PR) is defined as:

$$PR = \frac{\text{Total amount of both enantiomers in respective fractions}}{\text{(Mass of stationary phase)(cycle time)}} = \frac{V_{inj}}{w_{csp} t_c}[c_{inj,R} Y_{\mathrm{R}} + c_{inj,S} Y_{\mathrm{S}}] \tag{10}$$

where V_{inj} is the injection volume, $c_{inj,i}$ is the injection concentration of component i, w_{csp} and t_c are the mass of stationary phase and cycle time respectively. The cycle time is defined as the minimum time interval between two continuous injections and is equal to $t_{\mathrm{S}}^{\mathrm{end}} - t_{\mathrm{R}}^{\mathrm{start}}$.

In chromatographic separations, product recovery and solvent handling both contribute to the cost of separation. In SFC where a modified mobile phase is used, it is important to carefully define the solvent consumption. While the chromatographic separation itself is carried out at high pressure, the product is collected at low pressure. Under these conditions, the CO_2 is evaporated while the solute, along with the modifier is collected. In the next step, the solute is separated from the modifier typically through evaporation. Compared to the pumping of the mobile phase, evaporation is more energy intensive and only the amount of modifier in the product contributes to the cost. Hence in this work, the solvent consumption (S) is defined as the volume of modifier required per kg of the product produced:

$$S = \frac{\text{Total amount of modifier used in one cycle}}{\text{Total amount of both enantiomers collected in one cycle}} = \frac{Q_{mod} t_c}{V_{inj}[c_{inj,R} Y_{\mathrm{R}} + c_{inj,S} Y_{\mathrm{S}}]} \tag{11}$$

where Q_{mod} is the volumetric flow rate of modifier.

4.2 Choice of cut time

In preparative chromatography, the choice of collection intervals is crucial to maintain product quality and performance of the process. In general, when the mixture to be separated consists of two components in comparable quantities, a strategy has to be developed for choosing collection windows. The current work is limited to a binary separation and it is assumed that peaks from consecutive injections are at least baseline separated. In other words, only

the peaks of the two components from a particular injection are allowed to overlap. Further, only two fractions are collected and the recycle of impure fractions is not considered.

A simulated chromatogram is shown in Fig. 3 in order to explain the fraction collection strategy. In order to illustrate the general methodologies, a simulation where the peaks of the two components overlap is shown. The selection of $t_{\mathrm{R}}^{\mathrm{start}}$, the time at which the fraction containing R starts and $t_{\mathrm{S}}^{\mathrm{end}}$, the time at which the fraction containing S ends are rather straightforward. They are defined as the place where the concentration is 1% of the peak value. However, the choice of $t_{\mathrm{R}}^{\mathrm{end}}$ and $t_{\mathrm{S}}^{\mathrm{start}}$ require attention. If the expected purities are equal to 100% then this can be achieved by selecting $t_{\mathrm{R}}^{\mathrm{end}} = t_s$ and $t_{\mathrm{S}}^{\mathrm{start}} = t_r$ as shown in Fig. 3, where t_s corresponds to the time at which S starts eluting and t_r corresponds to the time at which R has fully eluted. It is worth noting that although this results in 100% purities, the recovery is compromised as the fraction between t_r and t_s is not collected. For cases, where purity requirement is less than 100%, the following strategy is used. Herein, $t_{\mathrm{R}}^{\mathrm{start}}$ and $t_{\mathrm{S}}^{\mathrm{end}}$ are fixed as discussed above. An arbitrary cut time,t_x with $t_{\mathrm{R}}^{\mathrm{start}} < t_x < t_{\mathrm{S}}^{\mathrm{end}}$, is then chosen. It can be seen that shifting t_x from t_s to t_r results in decreasing the purity of R but increasing the purity of S. Therefore, there exist a point (t_p) where purities of two components are equal (P_{R}=P_{S}=P_p). Under these circumstances, three possible scenarios can be expected based on the related values of P_p and the required purity P_{req}:

(1) If $P_p > P_{req}$, to keep high recovery, only a single cut is made and t_x is chosen in such a way that the purity requirements are satisfied.
(2) If $P_p = P_{req}$, t_x is set to the position of t_p.
(3) If $P_p < P_{req}$, one cut can not fulfill purity constraint and two cuts (t_{x1}, t_{x2}) that satisfy the respective purity constraints are made. This scenario will result in three fractions of which two are collected. The middle fraction, i.e. between t_{x1} andt_{x2}, is not recycled.

It is worth pointing out that the above strategy is suitable where the purity requirement on both components are identical, a case that is considered in this study.

4.3 Formulation of optimization problem

Optimization problems can be sorted into two kinds with respect to the number of objective functions, namely single and multi-objective. These two kinds of optimization problems are conceptually different. Single objective problems seek to maximize or minimize one objective function and result in an unique set of decision variables. In the case of multi-objective optimization there may

not be an unique optimum (i.e., a single point) with respect to all the objectives. Instead, there would be an entire set of optimal solutions (i.e., a curve) known as Pareto curve when the objectives conflict with each other. For example, in preparative chromatography, it is desired to maximize productivity but minimize solvent consumption. Every point on the Pareto curve is an optimal solution since moving from one point to another only one objective function improves whereas all others deteriorate. The final choice of an optimal Pareto point at which the process will be operated depends on relative cost of the two objectives.

In SFC the availability of a large number of operating parameters make the optimization problems challenging. As a matter of fact, although multi-objective optimization for single column and multi-column chromatography and hybrid processes are available [17–21], an optimization study of the SFC process is rare in the literature. It is well known that appropriate formulation of the optimization problem is the most crucial part in an optimization study. Since the economics of the SFC process has opposite interests in terms of solvent consumption and productivity, the optimization for SFC can properly be set as a two objective optimization problem with the aim of minimization of the solvent consumption and maximization of the productivity.

Objective functions are functions of decision variables which are selected as the operating parameters, i.e., separation conditions that significantly influence the process performance. In this study, injection volume (V_{inj}), injection concentration of the solutes to be separated (c_{inj}), modifier concentration (c_m) and mass flow rate of CO_2 (m_{CO_2}) have been chosen as the decision variables while the system back pressure has been set to 135 bar and the temperature is set to 30°C.

The solution to an optimization problem must satisfy one or several constraints defined in the space of objectives or decision variables. The constraints can be either from the limitation of the equipment or from the production requirement. Two kinds of constraints were used in this study. One is the physical limitation, namely, maximum pressure drop which the stationary phase can withstand and the solubility of solute in mobile phase. The others concern the quality of the product namely, recovery and purity. The physical limitation is a "hard" constraint since the equipment cannot be operated above such condition. Recovery and purity are "soft" constraints. Since the optimization is carried out over a range of recovery and purity values, the ranges of the decision variables are decided considering the equipment limitation such as available sample loop volume and applicable range of isotherm data. The complete description of the optimization problem is given in Tables 2 and 3. It is worth noting that, although we present results for a specific system (flurbiprofen), the analysis bears general applicability.

There are several methods to solve multi-objective optimization problem. In this work, non-dominated sorting generic algorithm (NSGA), a modified version of simple GA is used [21]. Non-domination refers to a better solution than another in at least one objective. The mutation and crossover operators are the same as simple GA. A random or given seed is used as the first generation. Upon mutation and crossover, the next generation is generated and sorted according to the fitness of the solution. Such steps are repeated for a pre-set number of generations to obtain the optimal solution. Compared to a single objective optimization algorithm such as Simplex, NSGA guarantees escape from converging into a local optimum. The parameters used by NSGA for all the optimization runs are listed in Table 4.

5 Results and discussion

5.1 Optimal Pareto curves

The multi-objective optimization of SFC was solved for four purity requirements namely, 95, 97, 99, 100%. For 95, 97, 99 %, a minimum recovery of 95% is set as a constraint and for purity of 100%, the recovery constraint is set to 100%. The resulting Pareto curves are shown in Fig. 4 where the axes correspond to the two objective functions, namely productivity and solvent consumption. As a general trend, with decreasing product purity requirement, it is observed that the Pareto curves move down and right indicating lower solvent consumption and higher productivity.

As observed, for total separation, a steep Pareto curve was obtained which indicates that an increase in productivity is possible only at the expense of solvent consumption. This is due to the rather high product quality requirement. When decreasing the purity requirement, the slopes of Pareto curves decrease indicating an operating range where improvement in productivity can be achieved without compromising much for the solvent consumption. Figure 4 enables us to calculate required solvent amount for a fixed productivity value. For example, for a productivity of 5 kg/kg/day, 80 L/kg rac of solvent will be necessary for both purity and recovery of 95%. It is worth emphasizing that liquid phase SMB separations which typically have comparable productivities result in much higher solvent consumption [22]. These results provide strong motivation for practitioners to consider SFC as a powerful alternative.

5.2 Effect of decision variables on process performance

An optimal solution is a set of best decision variables searched by the optimization algorithm. An understanding of how each decision variable affects the separation performance will yield better understanding of the process. A detailed discussion of the effects of the decision variables on isocratic SFC separation process is presented below.

5.2.1 Modifier concentration, c_m

To elute a polar solute, a highly polar organic solvent such as methanol or ethanol is usually added to the mobile phase. With addition of a modifier, the solute normally elutes earlier compared to the use of pure CO_2 as an eluent since the modifier can either increase the solubility and/or directly compete for the adsorption sites with solute. The effect of modifier concentration on productivity and solvent consumption in this study is shown in Fig. 5. It is clear from Fig. 5 that in general, most of the optimal operating points lie close to the upper bound of this decision variable. However, for the case of 100% purity, it is seen that increasing modifier composition leads to increased productivity. This trend is because of the fact that the addition of modifier reduces the elution time of enantiomers thus decreasing the cycle time.This is an important observation and rather counter-intuitive. It would be expected that an increased modifier concentration will also lead to an increased solvent consumption. However, the optimization results indicate that the possibility to inject larger concentrations owing to a larger solubility and the reduction in cycle time owing to an increased modifier composition results in a reduced solvent consumption. It is worth pointing out that these results should be viewed in the light that only a limited range of c_m has been used in this study and exploring larger modifier compositions, in the future, could be beneficial.

5.2.2 Throughput parameters,V_{inj}, c_{inj}

Throughput parameters include injection volume and injection concentration. High injection amount of solute can be achieved either by high concentration with small injection volume (concentration overloading) or by injecting large volume with low concentration of solute (volume overloading). In this study, both injection volume and concentration have been used as decision variables to investigate the optimal injection conditions. This plot confirms an intuitive understanding that higher injection concentrations lead to better process performance. The effect of injection concentration on the process performance is shown in Fig. 6. There appears to be no clear trend with respect to this decision variable, except for the case of purity = 100% where larger injection

concentrations lead to increased productivity and solvent consumption. Figure 7 shows the plot of c_{inj} vs c_m for the points on the Pareto. It is worth observing that most of the optimal points indeed lie close to the solubility limit. The effect of injection volume is shown in Fig. 8. It is observed that increasing injection volume caused lower productivity and solvent consumption. When productivity was plotted against the total amount injected in Fig. 9 ($n_{inj} = c_{inj}v_{inj}$), clear trends are seen. Smaller injection amounts tend to favor high productivity but result in increased solvent consumption. It is also seen that the solvent consumption for all cases seem to fall on a curve. This trend is a result of the definition of the solvent consumption which is based on the amount of solute injected.

5.2.3 Effect of flow rate

Flow rate is a key decision variable and it is easy to manipulate. In the current study, the mass flow rate of CO_2 was selected as decision variable and the modifier was added accordingly to provide desired value of c_{m}. The effect of flow rate on productivity and solvent consumption is shown in Fig. 10. It is clear from the figure that high flow rate results in an increase in productivity and solvent consumption. However, the upper limit for increasing the flow rate is determined by the maximum pressure drop.

6 Experimental implementation of optimum conditions

Every Pareto point in Fig. 4 is associated with a set of decision variables. In order to demonstrate the validity of the optimization, two points from the Pareto curves (circled) (c.f. Fig. 4) were selected for experimental implementation on an analytical laboratory set-up. The elution profile shown in Fig.11 (a) corresponds to a situation where both purity and recovery are expected to be 100%. This requirement can be met only if the two components are baseline separated. Hence only two fractions will be obtained. The injection volume was 70μL, and the CO_2 flow rate was was 0.97 mL/min, close to conditions where the experiments for parameter estimation were performed. As seen from the figure, the experimental elution profile shows good agreement with the calculated one. The cut times suggested by the optimizer also indicate that pure fractions can indeed be collected. The existing facility in our laboratory limits fraction collection and hence check for purity was not performed.

The elution profile shown in Fig. 11 (b) corresponds to a situation where $Y_i = P_i = 95\%$ where baseline separation is not a pre-requisite. The values of the all the decision variables are provided in the caption of the figure. In this case the injected volume was 170μL and the CO_2 flow rate was 1.63 mL/min;

much larger than conditions at which the characterization experiments were performed. As seen from the figure, the experimental elution profile shows minor deviation compared to the calculated one, especially in the region where the two components overlap. These deviations could arise due to the simplifications in the modeling, such as use of a constant Γ_i, or minor loss of column efficiency. However, it is worth noting that times at which the elution profile begins and ends and the tail of the second component all compare very well with the calculated ones. These observations point to the fact that the optimization results can be directly translated into experimental separations.

7 Conclusions

In this study a general methodology for the rational design of SFC separations have been provided. This involves characterization at analytical scale; estimation of process parameters and process design based on multi-objective optimization. The characterization experiments showed that in the region that was explored the variation of HETP was minor allowing the use of high flow rates. The maximum flow rate in SFC, seems to the governed by the resulting pressure drop than the loss of column efficiency. It was shown that the larger modifier compositions resulted in improving process performance both in terms of productivity and solvent consumption. The effect of different operating parameters yielded general characteristics that can be useful for practitioners to develop general heuristics for rapid scale-up of preparative SFC separations. Finally, two points from the Pareto curves were chosen for experimental implementation. The experimental elution profiles compared well with the calculated ones demonstrating the reliability of optimization results.

8 Notation

a	parameter in Henry constant correlation in Equation 3 [-]
c	fluid phase concentration of solute [g L^{-1}]
c_{inj}	injected concentration [g L^{-1}]
c_{m}	modifier concentration [w/w]
D_{ax}	axial dispersion coefficient [cm^2 s^{-1}]
d	parameter in Henry constant correlation in Equation 3 [-]
H	Henry constant [-]
K	equilibrium constant in Langmuir isotherm [L g^{-1}]
L	column length [cm]
k_f	mass transfer coefficient [s^{-1}]
m	mass flow rate [g s^{-1}]

n	solid phase concentration of solute [g L^{-1}]
n^*	equilibrium solid-phase concentration of solute [g L^{-1}]
P	purity [%]
PR	productivity [kg/kg/day]
p	parameter in Henry constant correlation in Equation 3 [-]
ΔP	pressure drop [bar]
Q	volumetric flow rate [cm^3 min^{-1}]
q	parameter in Henry constant correlation in Equation 3 [-]
S	solvent consumption [L kg^{-1}]
t	time [s]
t_c	cycle time [s]
v	interstitial velocity [cm s^{-1}]
V_{inj}	volume of injection loop [cm^3]
w_{csp}	mass of stationary phase [g]
Y	recovery [%]
z	axial coordinate [cm]

443 Subscripts and Superscripts

cal	calculation
exp	experiment
i	components
mod	modifier
min	minimum
R	enantiomer R
req	required
S	enantiomer S

444 Greek symbols

β	Column permeability [m mL^{-1}]
ϵ	void fraction of column [-]
μ	viscosity [Pa s]
ρ	density [g L^{-1}]
σ	solubility [g L^{-1}]
Γ	saturation capacity [g L^{-1}]

445 **References**

446 [1] US Food and Drugs Administration, Drugs, *Chirality* 4 (1992) 338–340.

[2] S. Erb, *Pharm. Technol.* 30 (2006), p. s14.

[3] G. Guiochon, *J. Chromatogr. A* 965 (2002) 129–161.

[4] A. Rajendran, G. Paredes, M. Mazzotti, *J. Chromatogr. A* 1216 (2009) 709–738.

[5] L. T. Taylor, *J. Supercrit. Fluids* 47 (2009) 566–573.

[6] T. A. Berger, R. S. of Chemistry (Great Britain), Packed column SFC, The Royal Society of Chemistry, Cambridge, 1995.

[7] C. J. Welch, W. R. Leonard Jr, J. O. DaSilva, M. Biba, J. Albaneze-Walker, D. W. Henderson, B. Laing, D. J. Mathre, R. E. Majors, *LC-GC North America* 23 (2005) 16–29.

[8] F. Denet, W. Hauck, R. M. Nicoud, O. Di Giovanni, M. Mazzotti, J. N. Jaubert, M. Morbidelli, *Ind. Engg. Chem. Res.* 40 (2001) 4603–4609.

[9] A. Depta, T. Giese, M. Johannsen, G. Brunner, *J. Chromatogr. A* 865 (1999) 175–186.

[10] A. Rajendran, S. Peper, M. Johannsen, M. Mazzotti, M. Morbidelli, G. Brunner, *J. Chromatogr. A* 1092 (2005) 55–64.

[11] G.J. Chin, Z.H. Chee, W. Chen, A. Rajendran, *J. Chem. Eng. Data* 55 (2010) 1542–1546.

[12] C. Wenda, A. Rajendran, *J. Chromatogr. A* 1216 (2009) 8750–8758.

[13] A. Rajendran, T. S. Gilkison, M. Mazzotti, *J. Sep. Sci.* 31 (2008) 1279–1289.

[14] A. Rajendran, O. Kräuchi, M. Mazzotti, M. Morbidelli, *J. Chromatogr. A* 1092 (2005) 149–160.

[15] K. Liu, E. Kiran, *Ind. Engg. Chem. Res.* 46 (2007) 5453–5462.

[16] A. Rajendran, M. Mazzotti, M. Morbidelli, *J. Chromatogr. A* 1076 (2005) 183–188.

[17] M. Amanullah, M. Mazzotti, *J. Chromatogr. A* 1107 (2006) 36–45.

[18] M. Amanullah, C. Grossmann, M. Mazzotti, M. Morari, M. Morbidelli, *J. Chromatogr. A* 1165 (2007) 100–108.

[19] G. Paredes, M. Mazzotti, *J. Chromatogr. A* 1142 (2007) 56–68.

[20] Z. Zhang, K. Hidajat, A. K. Ray, M. Morbidelli, *AIChE J.* 48 (2003) 2800–2816.

[21] Z. Zhang, M. Mazzotti, M. Morbidelli, *J. Chromatogr. A* 989 (2003) 95–108.

[22] J.R. Bruno, *Chim. Oggi* 22 (2004) 32–34.

9 List of Figure Captions

Figure 1:
Experimental (symbols) and calculated pressure drop by Equation 1(lines) under different CO_2 flow rates and modifier concentrations. Back pressure: 135 bar.

Figure 2:
Experimentally measured HETP values under different operating conditions. Symbols represent experimentally measured values while lines are drawn to show the trend.

Figure 3:
Illustration of strategy to decide cut time using a simulated chromatogram. R enantiomer is collected from $t_{\mathrm{R}}^{\mathrm{start}}$ to t_{x1} and S enantiomer is collected from t_{x2} to $t_{\mathrm{R}}^{\mathrm{end}}$ to ensure the constraints are satisfied. Insert shows the complete chromatogram. The cycle time is $t_{\mathrm{S}}^{\mathrm{end}}$-$t_{\mathrm{R}}^{\mathrm{start}}$.

Figure 4:
Pareto curves showing the trade-off between the two objective functions namely, productivity and solvent consumption under different purity and recovery constraints.

Figure 5:
The effect of modifier concentration on a) productivity and b) solvent consumption.

Figure 6:
The effect of injection concentration on a) productivity and b) solvent consumption.

Figure 7:
The solubility and optimal injection concentrations under different modifier compositions.

Figure 8:
The effect of injection volume on a) productivity and b) solvent consumption.

Figure 9:
The effect of injection amount on a) productivity and b) solvent consumption.

Figure 10:
The effect of CO_2 mass flow rate on a) productivity and b) solvent consumption.

Figure 11:
Comparison of experimental (symbols) and simulation results (lines) for optimal solution. a) Optimal operating condition for a constraint with $Y_i = P_i = 100\%$. CO_2 flow rate: 0.97 mL/min, c_{m}= 19.0%, back pressure: 135 bar, V_{inj}=70 μL, c_{inj}=111 g/L. b) Optimal operating condition for a constraint with $Y_i = 95\%$ and $P_i = 97\%$. CO_2 flow rate: 1.63 mL/min, c_{m}= 18.9%, back pressure: 135 bar, V_{inj}=170 μL, c_{inj}=121 g/L.

10 List of Table Captions

Table 1:
Adsorption isotherm parameters, corresponding to Eq. 2 and 3, reference density $\rho^0 = 1000.0$ g L^{-1}

Table 2:
Objective functions and constraints for the optimization study.

Table 3:
Range of values for decision variables.

Table 4:
Parameters of NSGA used in multi-objective optimization study.

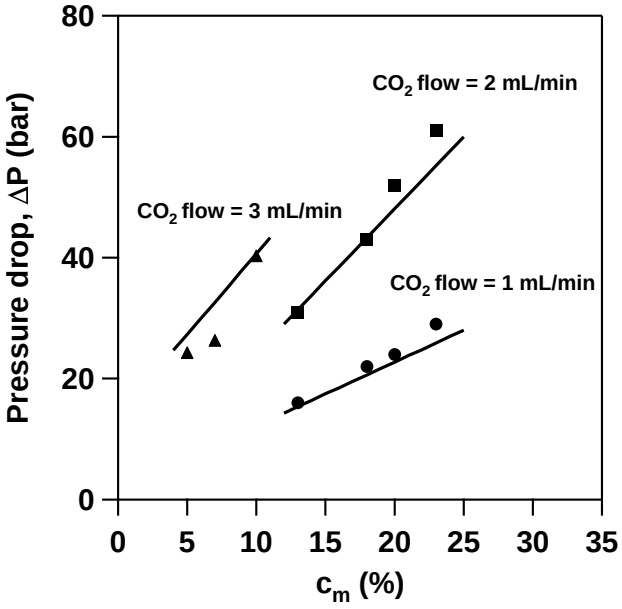

Fig. 1. Experimental (symbols) and calculated pressure drop by Equation 1(lines) under different CO_2 flow rates and modifier concentrations. Back pressure: 135 bar.

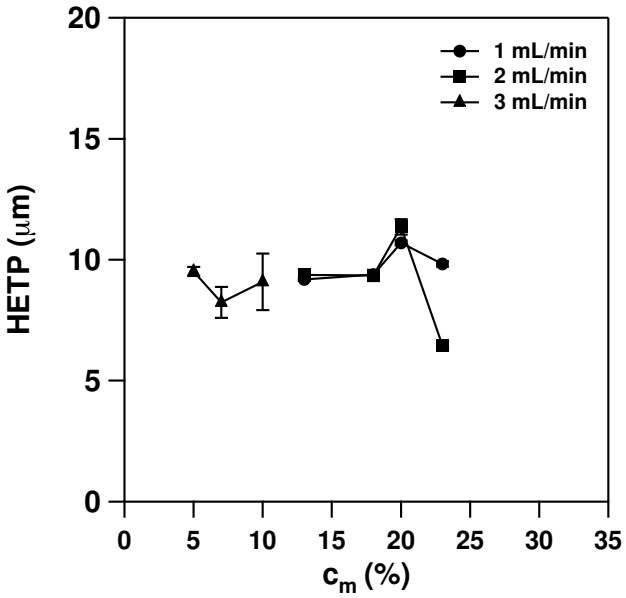

Fig. 2. Experimentally measured HETP values under different operating conditions. Symbols represent experimentally measured values while lines are drawn to show the trend.

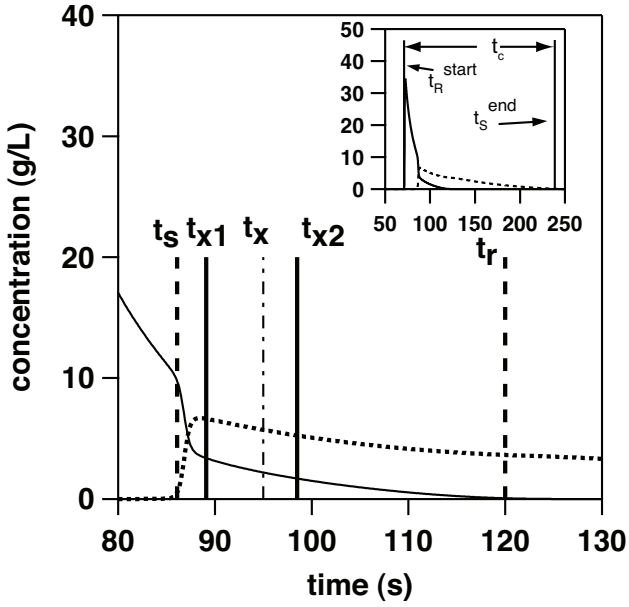

Fig. 3. Illustration of strategy to decide cut time using a simulated chromatogram. R enantiomer is collected from $t_{\mathrm{R}}^{\mathrm{start}}$ to t_{x1} and S enantiomer is collected from t_{x2} to $t_{\mathrm{R}}^{\mathrm{end}}$ to ensure the constraints are satisfied. Insert shows the complete chromatogram. The cycle time is $t_{\mathrm{S}}^{\mathrm{end}}$-$t_{\mathrm{R}}^{\mathrm{start}}$

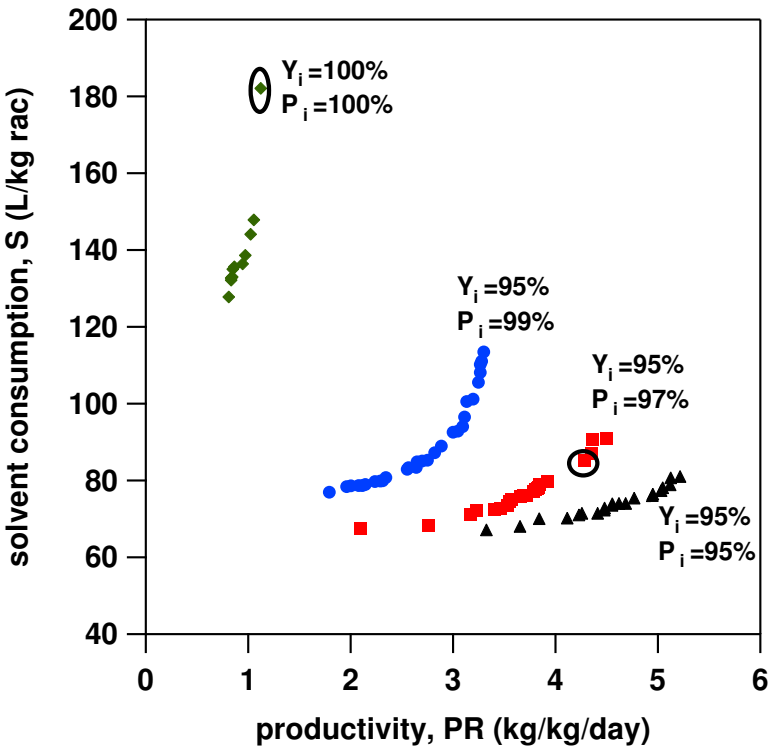

Fig. 4. Pareto curves showing the trade-off between the two objective functions namely, productivity and solvent consumption under different purity and recovery constraints.

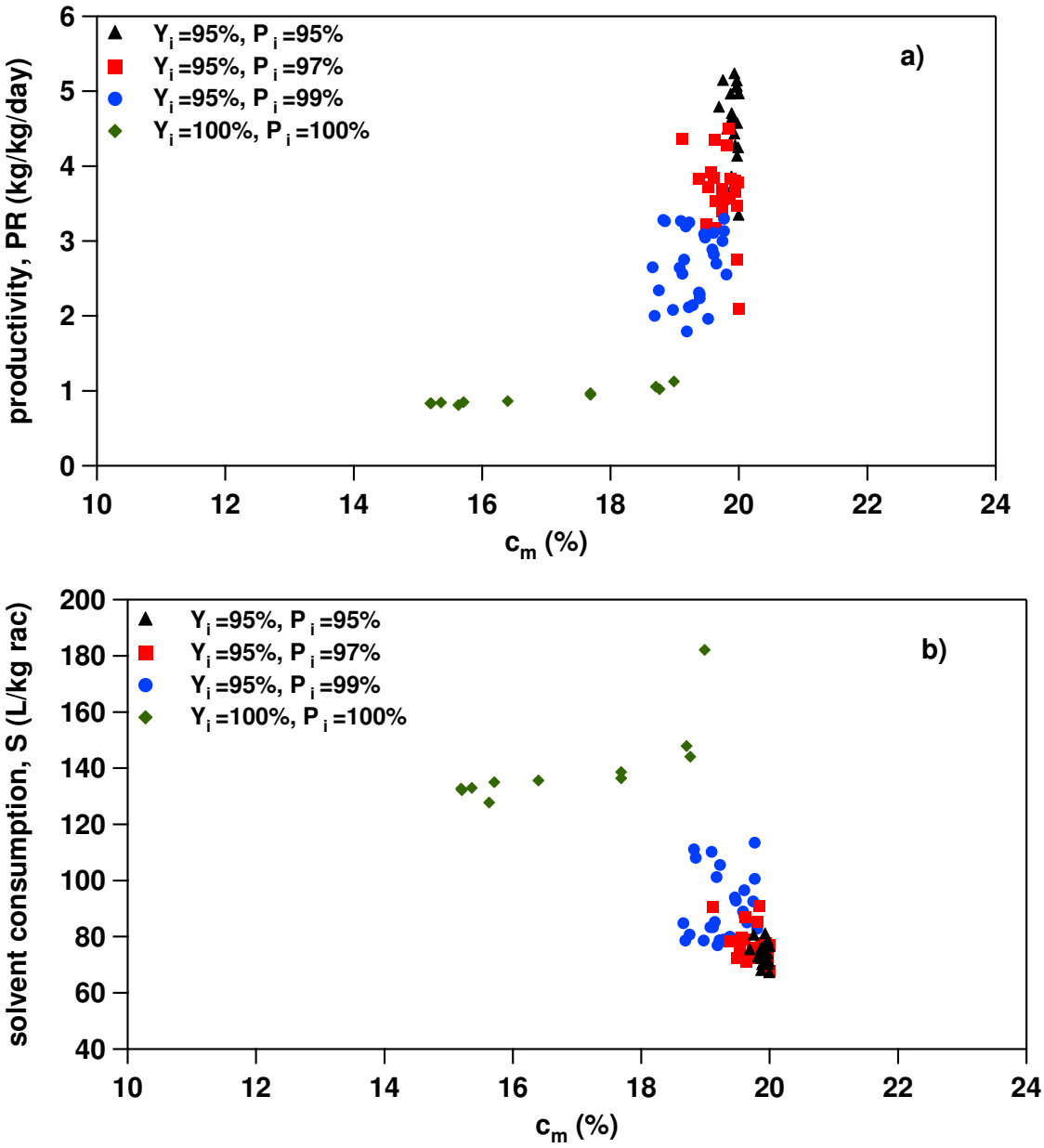

Fig. 5. The effect of modifier concentration on a) productivity and b) solvent consumption.

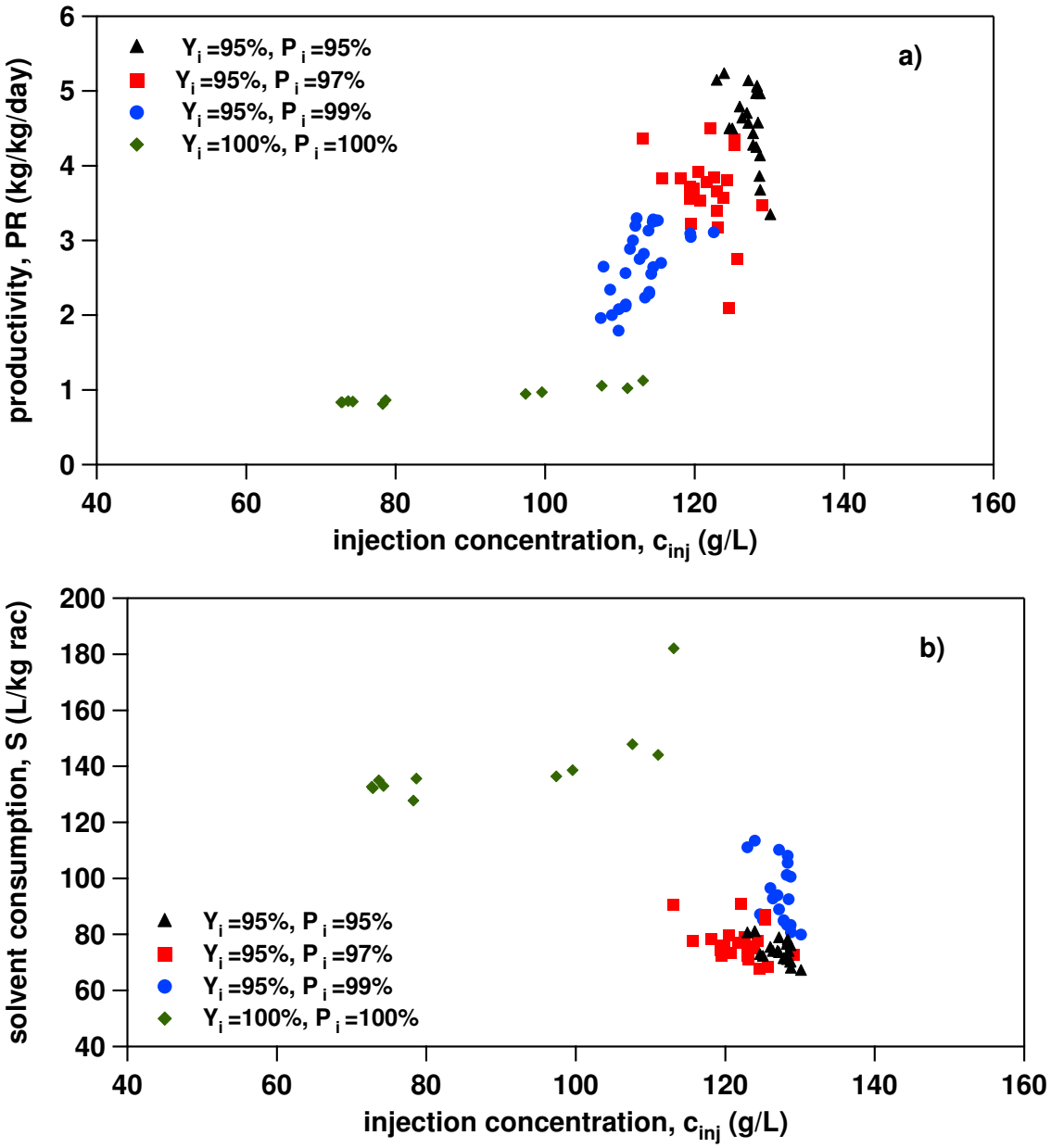

Fig. 6. The effect of injection concentration on a) productivity and b) solvent consumption.

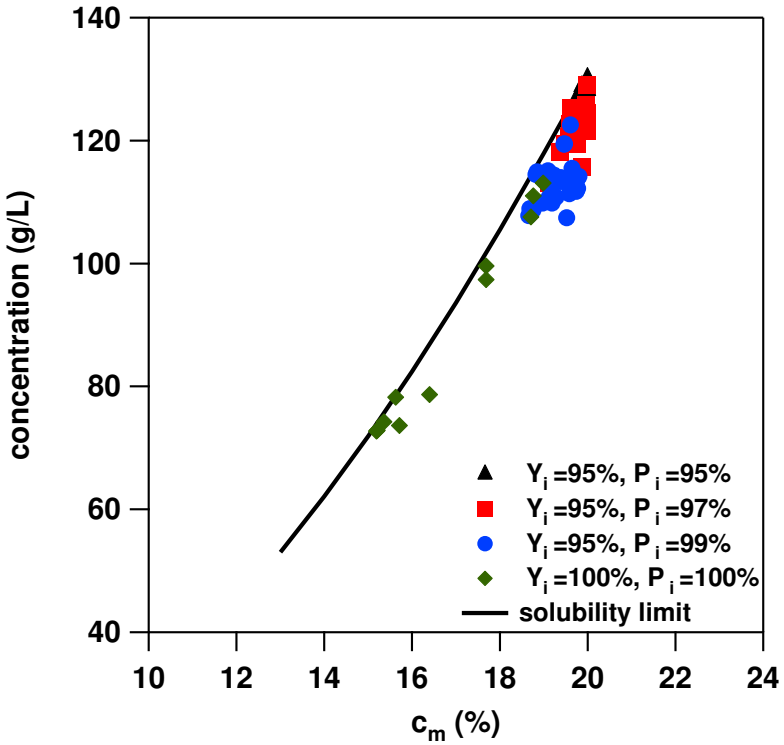

Fig. 7. The solubility and optimal injection concentrations under different modifier compositions.

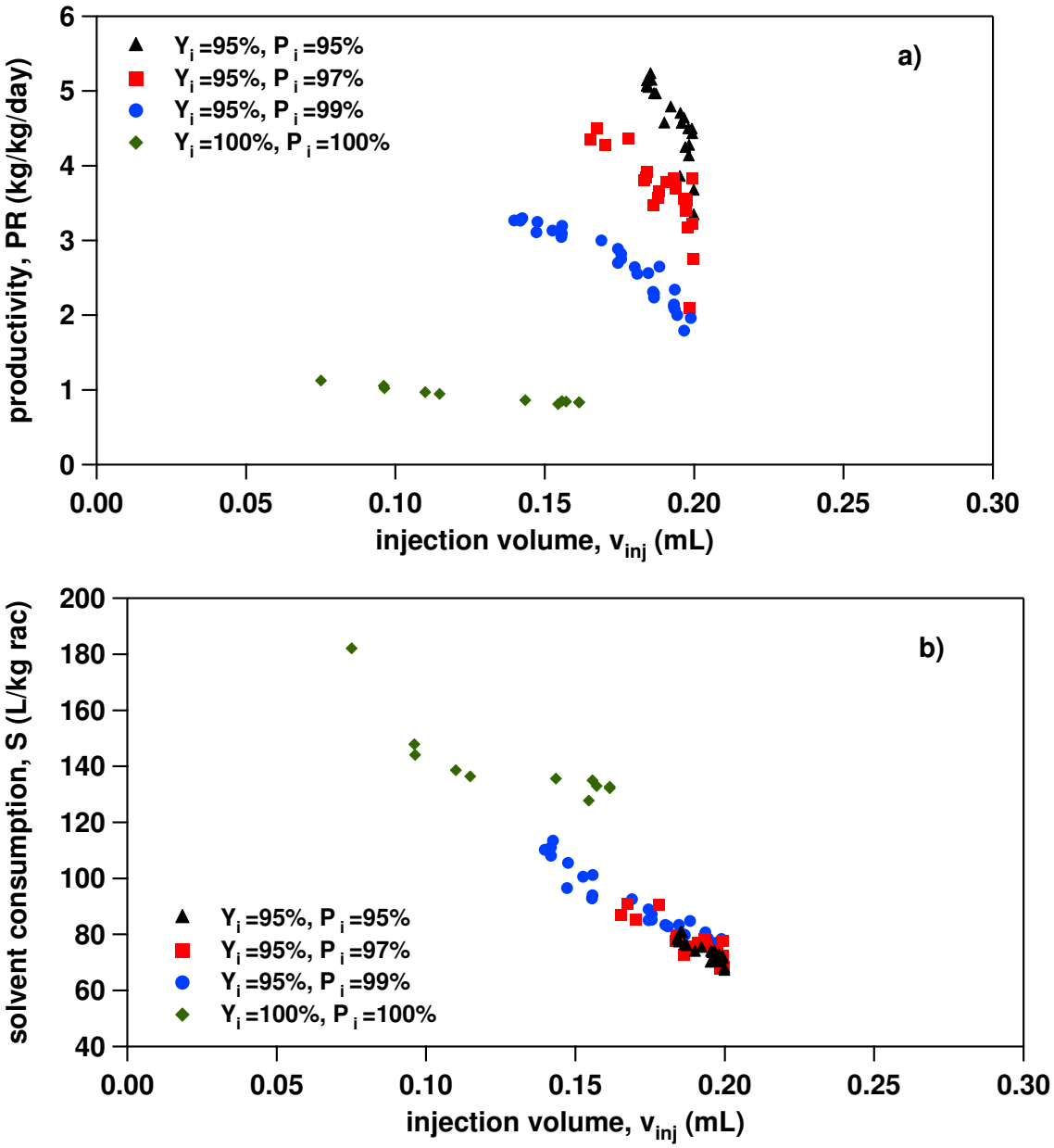

Fig. 8. The effect of injection volume on a) productivity and b) solvent consumption.

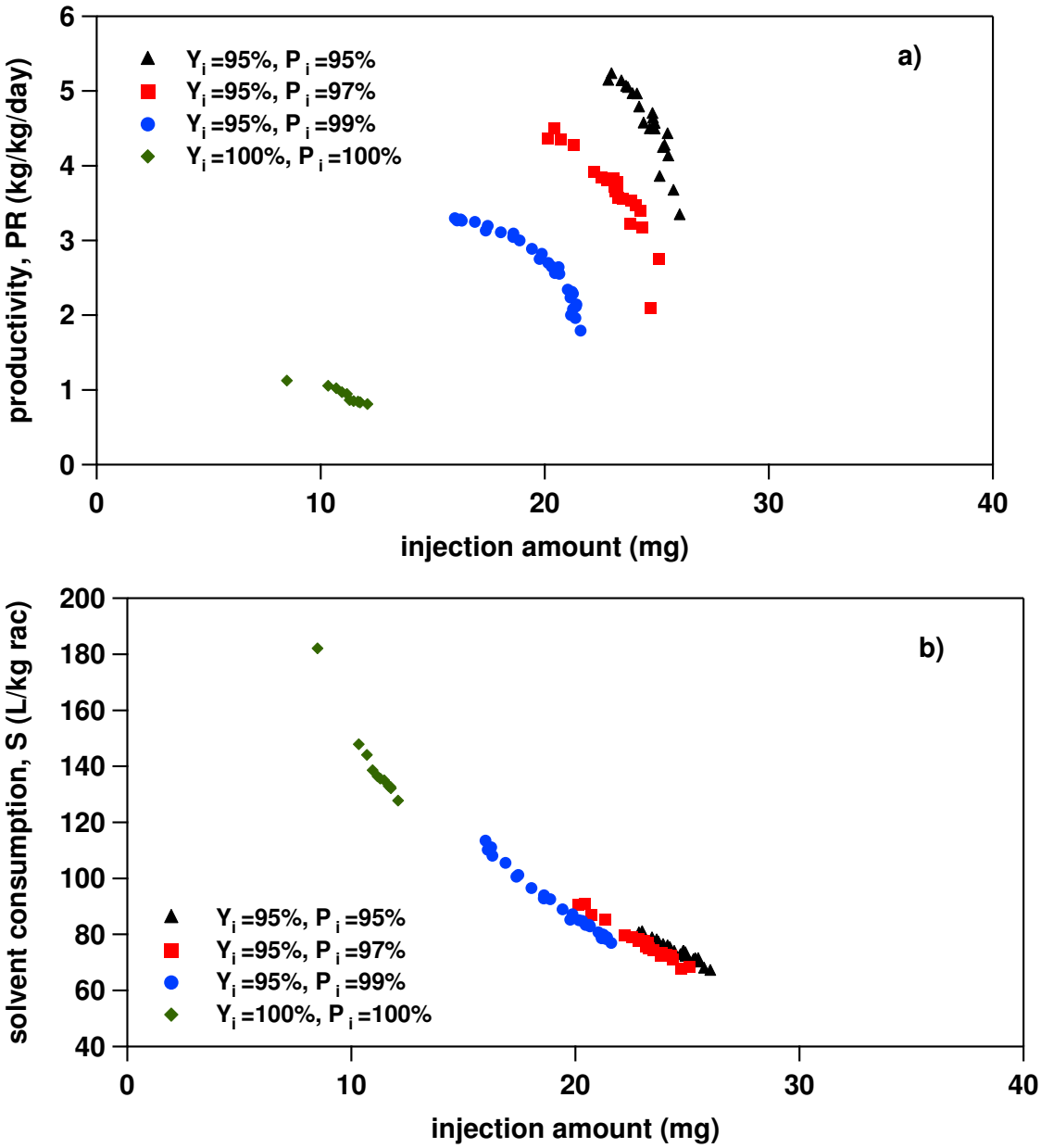

Fig. 9. The effect of injection amount on a) productivity and b) solvent consumption.

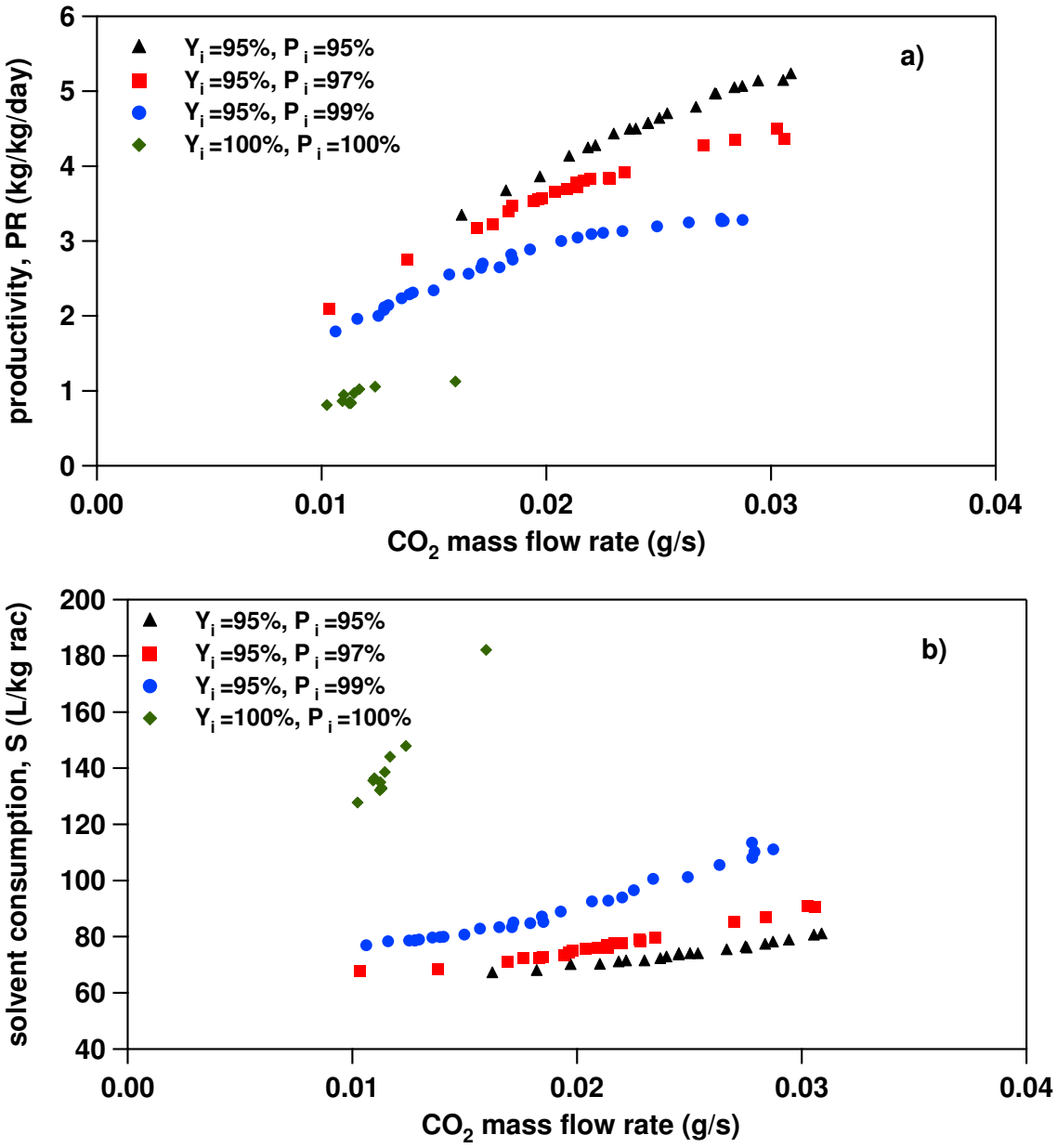

Fig. 10. The effect of CO_2 mass flow rate on a) productivity and b) solvent consumption.

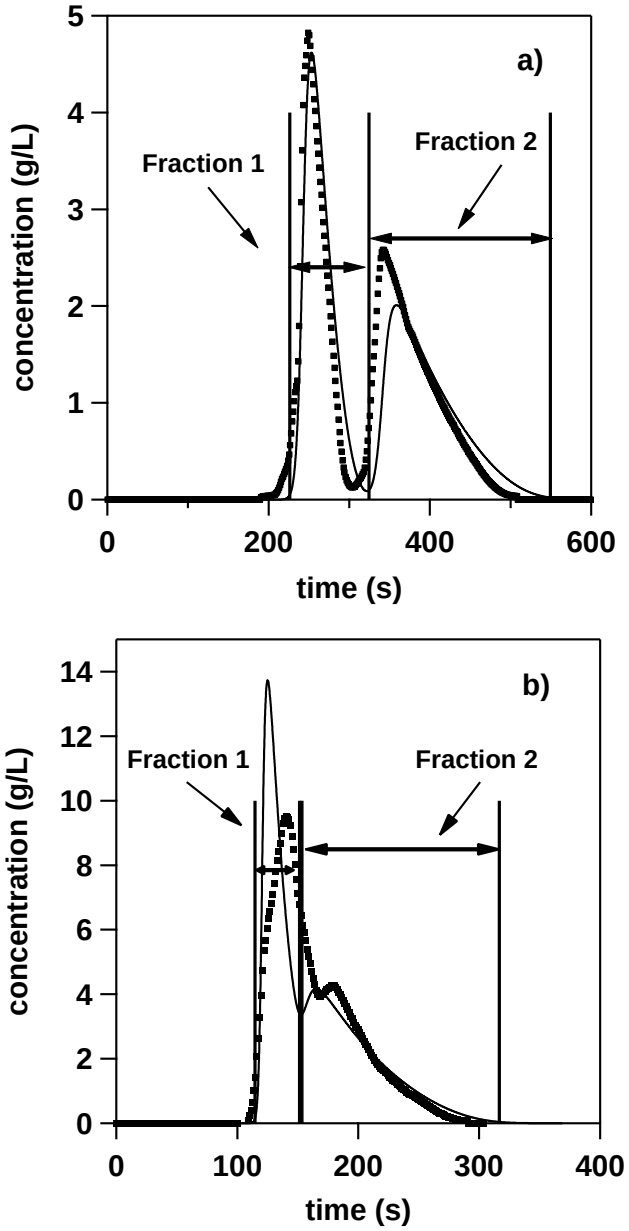

Fig. 11. Comparison of experimental (symbols) and simulation results (lines) for optimal solution. a) Optimal operating condition for a constraint with $Y_i = P_i = 100\%$. CO_2 flow rate: 0.97 mL/min, c_{m}= 19.0%, back pressure: 135 bar, V_{inj}=70 μL, c_{inj}=111 g/L. b) Optimal operating condition for a constraint with $Y_i = 95\%$ and $P_i = 97\%$. CO_2 flow rate: 1.63 mL/min, c_{m}= 18.9%, back pressure: 135 bar, V_{inj}=170 μL, c_{inj}=121 g/L.

Table 1
Adsorption isotherm parameters, corresponding to Eq. 2 and 3, reference density ρ^0 = 1000.0 g L^{-1}

Component	a	d	p	r	Γ [g/L]
R	0.0242	-0.137	0.0165	1.74	102.0
S	0.0105	-0.0382	0.0794	4.94	75.0

Table 2
Objective functions and constraints for the optimization study.

Objective functions	1. Max: PR(v_{inj}, c_{inj}, c_m, m_{CO_2})
	2. Min: S(v_{inj}, c_{inj}, c_m, m_{CO_2})
Constraints	1. P=x± 0.002, x=95%, 97%, 99%,100%
	2. Y=y±0.002, y=95%,100%
	3. ΔP $\leq$50 bar
	4. c_{inj} $\leq$Solubility in mobile phase

Table 3
Range of values for decision variables.

Decision variable	Range
c_{inj}	5 - 200 g/L
V_{inj}	0.05 - 0.2 mL
c_m	13.0 - 20.0 % [w/w]
m_{CO_2}	0.01 - 0.1 g/s

Table 4
Parameters of NSGA used in multi-objective optimization study.

Parameters	Value
Number of generations	60
Population size	400
String length	24
Crossover probability	0.20
Mutation probability	0.05